OPEN ACCESS
CellPress

Cell Reports
Article

Peripheral Androgen Receptor Gene Suppression Rescues Disease in Mouse Models of Spinal and Bulbar Muscular Atrophy

Andrew P. Lieberman,[1,*] Zhigang Yu,[1] Sue Murray,[2] Raechel Peralta,[2] Audrey Low,[2] Shuling Guo,[2] Xing Xian Yu,[2] Constanza J. Cortes,[3] C. Frank Bennett,[2] Brett P. Monia,[2] Albert R. La Spada,[3,4] and Gene Hung[2,*]
[1]Department of Pathology, University of Michigan Medical School, Ann Arbor, MI 48104, USA
[2]Isis Pharmaceuticals, Inc., Carlsbad, CA 92010, USA
[3]Departments of Cellular and Molecular Medicine, Neuroscience, and Pediatrics, Institute for Genomic Medicine, and Sanford Consortium for Regenerative Medicine, University of California, San Diego, La Jolla, CA 92037, USA
[4]Division of Genetics/Dysmorphology, Rady Children's Hospital, San Diego, CA 92037, USA
*Correspondence: liebermn@umich.edu (A.P.L.), ghung@isisph.com (G.H.)
http://dx.doi.org/10.1016/j.celrep.2014.02.008

SUMMARY

Spinal and bulbar muscular atrophy (SBMA) is caused by the polyglutamine androgen receptor (polyQ-AR), a protein expressed by both lower motor neurons and skeletal muscle. Although viewed as a motor neuronopathy, data from patients and mouse models suggest that muscle contributes to disease pathogenesis. Here, we tested this hypothesis using AR113Q knockin and human bacterial artificial chromosome/clone (BAC) transgenic mice that express the full-length polyQ-AR and display androgen-dependent weakness, muscle atrophy, and early death. We developed antisense oligonucleotides that suppressed AR gene expression in the periphery but not the CNS after subcutaneous administration. Suppression of polyQ-AR in the periphery rescued deficits in muscle weight, fiber size, and grip strength, reversed changes in muscle gene expression, and extended the lifespan of mutant males. We conclude that polyQ-AR expression in the periphery is an important contributor to pathology in SBMA mice and that peripheral administration of therapeutics should be explored for SBMA patients.

INTRODUCTION

Spinal and bulbar muscular atrophy (SBMA) is one of nine untreatable diseases caused by CAG/glutamine tract expansions. In SBMA, a polyglutamine (polyQ) tract near the amino terminus of the androgen receptor (AR) leads to hormone-dependent protein unfolding and to the loss of lower motor neurons in the brainstem and spinal cord of affected males (Lieberman and Fischbeck, 2000). Clinical onset occurs in adolescence to adulthood and is characterized initially by muscle cramps and elevated serum creatine kinase (Katsuno et al., 2006b; Sperfeld et al., 2002). These myopathic features commonly precede muscle weakness, which inevitably develops as the disease progresses and is most severe in the proximal limb and bulbar muscles. As with all of the polyglutamine disorders, the mechanisms that lead to selective neuronal dysfunction and degeneration are poorly understood, and disease-modifying therapies are currently unavailable.

Several general principles have emerged from the study of SBMA model systems that guide our understanding of disease pathogenesis. Binding of testosterone or dihydrotestosterone to the polyQ-AR promotes ligand-dependent unfolding and nuclear translocation of the mutant protein (Katsuno et al., 2002; Takeyama et al., 2002). These steps are required for pathogenesis and underlie the occurrence of disease only in men. The mutation leads to a partial loss of transactivation function (Chamberlain et al., 1994; Irvine et al., 2000; Kazemi-Esfarjani et al., 1995; Lieberman et al., 2002; Mhatre et al., 1993), and while this may contribute to features of androgen insensitivity, neuromuscular degeneration is mediated by a toxic gain of function conferred by protein unfolding. In SBMA, as in other CAG/polyQ disorders, the mutant protein disrupts multiple downstream pathways, and toxicity likely results from the cumulative effects of altering a diverse array of cellular processes including transcription, RNA splicing, axonal transport, and mitochondrial function (Katsuno et al., 2006a; Kemp et al., 2011; McCampbell et al., 2000; Morfini et al., 2006; Ranganathan et al., 2009; Szebenyi et al., 2003; Yu et al., 2009). The existence of divergent mechanisms of toxicity suggests that potential treatments targeting a single downstream pathway are likely to be incomplete or unsuccessful. In contrast, efforts to target the polyQ-AR as the proximal mediator of toxicity by harnessing cellular machinery to promote its degradation hold promise for therapeutic intervention. Because the Hsp90-based chaperone machinery controls proteostasis of the AR (Morishima et al., 2008; Thomas et al., 2004, 2006; Wang et al., 2010), genetic and pharmacological approaches to promote Hsp70-dependent ubiquitination have been shown to facilitate degradation of the mutant protein (Wang et al., 2013).

Insights into the mechanisms underlying selective neuromuscular degeneration in SBMA have come from the study of mouse

models. Previous analysis of AR113Q knockin mice suggested that pathology arising in skeletal muscle contributes to the disease phenotype (Yu et al., 2006a). In these mice, denervation and myopathy precede spinal cord pathology, consistent with the notion that myopathy is an early disease manifestation (Jordan and Lieberman, 2008). Supporting a role for muscle in pathogenesis are data from transgenic mice that overexpress wild-type (WT) AR only in skeletal muscle and show hormone-dependent myopathy and motor axon loss (Johansen et al., 2009; Monks et al., 2007). That muscle both contributes to the SBMA phenotype and provides a therapeutic target is supported by data showing diminished disease severity in polyQ-AR transgenic mice with genetic overexpression of IGF-1 in skeletal muscle (Palazzolo et al., 2009) or with peripheral IGF-1 administration (Rinaldi et al., 2012).

Here, we test an alternative strategy to ameliorate toxicity in mouse models of SBMA by suppressing polyQ-AR expression using antisense oligonucleotides (ASOs). We use these compounds to specifically target polyQ-AR expression in the periphery. We demonstrate using two mouse models that peripheral gene suppression of the polyQ-AR rescues deficits in muscle weight, fiber size, and grip strength; reverses changes in muscle gene expression; and extends lifespan of mutant males. We conclude that polyQ-AR expression in the periphery is an important contributor to pathology in SBMA mice and that peripheral administration of therapeutics should be explored for SBMA patients.

RESULTS

Subcutaneous ASO Suppresses PolyQ-AR Expression in the Periphery but Not the Spinal Cord

We sought to define the contribution of peripherally expressed polyQ-AR to the phenotype of SBMA mice and to determine whether peripheral tissue is a therapeutic target. To accomplish this, we suppressed *AR* expression by subcutaneous administration of ASOs. Because these compounds do not cross the blood-brain barrier (Geary, 2009; Yu et al., 2007), this strategy selectively targeted *AR* in peripheral tissues such as skeletal muscle. We developed 16-mer chemically modified ASO complementary to human and mouse or human *AR* transcripts (ASO1 and ASO2 respectively; Table S1). These 2′,4′-constrained ethyl (cEt) gapmer ASOs show increased stability, tolerability, and potency upon in vivo administration (Seth et al., 2009). Initial characterization demonstrated dose-dependent suppression of human and mouse *AR* mRNAs in cell culture by targeted, but not control, ASOs (Figure 1A). Similarly, subcutaneous administration of targeted, but not control, ASOs led to dose-dependent suppression of *AR* mRNA and protein expression in skeletal muscle of WT male mice (Figures 1B and 1C). Serum testosterone levels of these males exhibited modest variability, and treatment with targeted ASOs did not result in a significant alteration (Figure S1).

We used these compounds to determine the extent to which suppressing peripheral expression of the polyQ-AR rescued the phenotype of SBMA mice. This was accomplished using both AR113Q knockin (Yu et al., 2006a; Yu et al., 2006b) and human bacterial artificial chromosome/clone (BAC) fxAR121 transgenic mice (Cortes et al., 2014). Both of these models express the full-length polyQ-*AR* under the regulation of its endogenous promoter. These mice display a similar androgen-dependent phenotype characterized by weakness, muscle atrophy, and early death. In both models, subcutaneous administration of ASOs decreased *AR* expression in skeletal muscle, but not spinal cord. To determine the targeting efficacy and specificity in skeletal muscle, BAC fxAR121 transgenic males were treated with the human *AR*-targeted ASO2. Subcutaneous administration of human *AR*-targeted ASO2, but not control ASO, led to dose-dependent suppression of transgene expression in skeletal muscle without affecting expression of the endogenous mouse allele (Figure 1D). While treatment with ASO2 (50 mg/kg, twice weekly, starting at 11 weeks) specifically suppressed transgene expression in skeletal muscle of BAC transgenic mice, the human and mouse cross-reactive ASO1 suppressed both transgenic human *AR* and endogenous mouse *AR* mRNA (Figure 2A), demonstrating target selectivity. Quantitative real-time RT-PCR demonstrated >95% reduction of human *AR* mRNA levels in skeletal muscle of treated males. No significant change in mouse or human *AR* mRNA levels was detected in brain or spinal cord of treated mice (Figure 2A), indicating that subcutaneous administration selectively targeted peripheral *AR* expression. The decrease of *AR* mRNA in muscle was associated with comparable reduction in AR protein immunoreactivity in skeletal muscle nuclei following treatment (Figure 2B).

AR113Q knockin males express a hybrid humanized *AR* in which most of mouse *AR* exon 1 has been replaced by human sequence (Yu et al., 2006b). Therefore, we used ASO1, a human and mouse *AR* cross-reactive ASO, to treat these mice. Subcutaneous administration of ASO1 (50 mg/kg, twice per week for 4 weeks and then once per week) or saline was initiated at 8 weeks and continued until 26 weeks. Treatment resulted in a significant decrease in *AR* mRNA levels in quadriceps muscle, but not spinal cord (Figure 2C). This decrease in *AR* expression was long-lived, as partial mRNA reduction was detected in skeletal muscle harvested from mice at 36 weeks of age, 10 weeks after the termination of treatment; by 46 weeks of age (20 weeks posttreatment washout), *AR* mRNA levels in muscle approached those of saline-treated controls. Similarly, sustained suppression of transcripts by ASOs has been reported in skeletal muscle of myotonic dystrophy mice (Wheeler et al., 2012). Knockdown of *AR* mRNA levels in muscle was associated with a ~90% decrease in AR protein levels (Figure 2D). We observed a slow recovery in AR protein levels in muscle after the termination of treatment, with expression remaining ~80% lower than controls at 10 weeks posttreatment and ~65% lower than controls at 20 weeks posttreatment (age 46 weeks). In contrast, *AR* mRNA and protein expression in spinal cord were not significantly altered by peripheral ASO delivery.

Peripheral PolyQ-AR Suppression Rescues Disease in SBMA Mice

Significant amelioration of disease phenotype following *AR* gene suppression in the periphery was observed in both SBMA mouse models. BAC fxAR121 mice exhibited an age-dependent loss of grip strength and body mass (Figures 3A

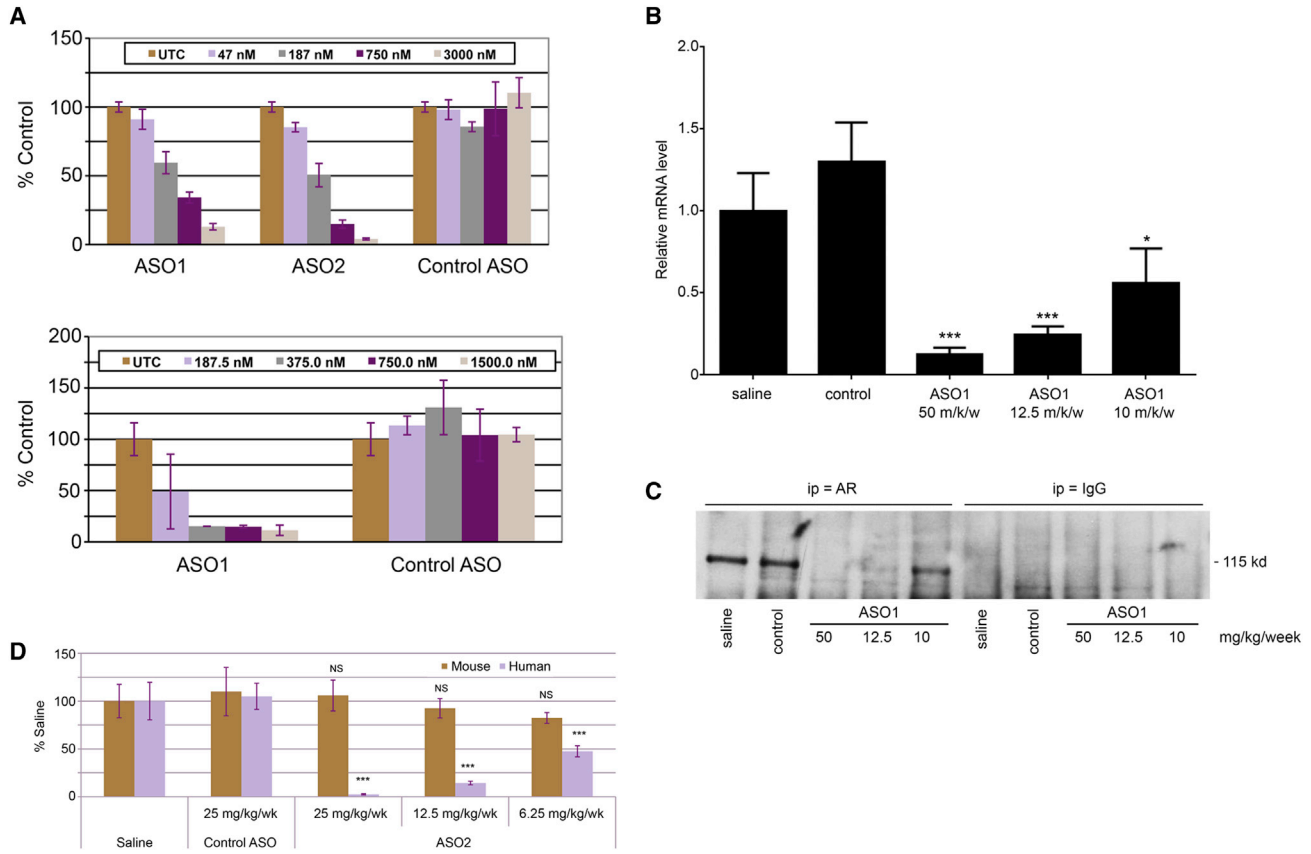

Figure 1. Dose-Dependent Suppression of AR Expression by Targeted ASOs

(A) Human umbilical vein endothelial cells (top) and mouse brain endothelial cells (bEnd.3) cells (bottom) were electroporated in the presence of *AR*-targeted or control ASOs at the indicated concentrations. Relative *AR* mRNA levels were determined after 16 hr and are reported as mean ± SD. UTC, untransfected control.

(B and C) Wild-type male mice received subcutaneous injections of ASO1, control ASO, or saline from 6 to 14 weeks (n = 3 per group). Animals were treated with ASO1 or control ASO at 50 mg/kg per week, or with two lower doses of ASO1 (25 mg/kg per day × 3 days, then 12.5 mg/kg per week; or 17.5 mg/kg per day × 3 days, then 10 mg/kg per week). Quadriceps muscle was harvested at 14 weeks for analysis of AR expression.

(B) Relative *AR* mRNA levels (mean ± SEM). *$p < 0.05$, ***$p < 0.001$.

(C) AR protein as detected by immunoprecipitation and western blot.

(D) BAC fxAR121 males (n = 4 per group) received subcutaneous injections of control ASO (25 mg/kg per week), ASO2 (25, 12.5, or 6.25 mg/kg per week), or saline from 7–15 weeks. Quadriceps muscle was harvested 48 hr after the final dose and analyzed for human and mouse *AR* mRNA levels. Data are mean ± SD. ***$p < 0.001$ compared to saline treatment.

and 3B). These deficits were partially rescued in a dose-dependent manner by subcutaneous administration of ASO2, but not control ASO (Figures 3A and 3B). Higher-dose treatment with ASO2 (50 mg/kg per week), starting at an asymptomatic age (6 weeks) and continuing for 4 weeks, completely ameliorated the loss of grip strength and body mass in transgenic males (Figures 3C and 3D). This was associated with rescue of lean body mass as measured by MRI (Figure 3E). BAC fxAR121 males treated with ASO2 showed a dose-dependent extension of lifespan (Figure 4A). Similarly, treatment of AR113Q knockin males with ASO1 starting at 8 weeks resulted in a significant extension of lifespan (Figure 4B), without altering serum testosterone levels (Figure S2).

To further assess the clinical implications and therapeutic relevance of this strategy, we initiated treatment with ASO2 in a separate cohort of BAC fxAR121 mice at 11 weeks, an age at which these males begin to exhibit diminished grip strength and body mass, as shown in Figure 3. Subcutaneous administration of ASO2 for durations varying from 2 to 8 weeks resulted in a significant increase in survival that reflected the length of treatment (Figure 5A). Furthermore, we detected a significant deficit in grip strength only in those animals treated with ASOs for the shortest duration (Figure 5B). These data indicate that therapeutic benefits from peripherally administered ASOs are dependent upon total treatment dose and are detected even when initiated at the onset of symptoms.

ASO treatment rescued polyQ-AR-mediated pathology in skeletal muscle of both SBMA mouse models. AR113Q knockin males showed skeletal muscle atrophy at 26 weeks of age, and both tibialis anterior muscle mass (Figure 6A) and quadriceps muscle fiber size (Figure 6B) were increased by ASO1 treatment starting at 8 weeks. This rescue of muscle mass was maintained

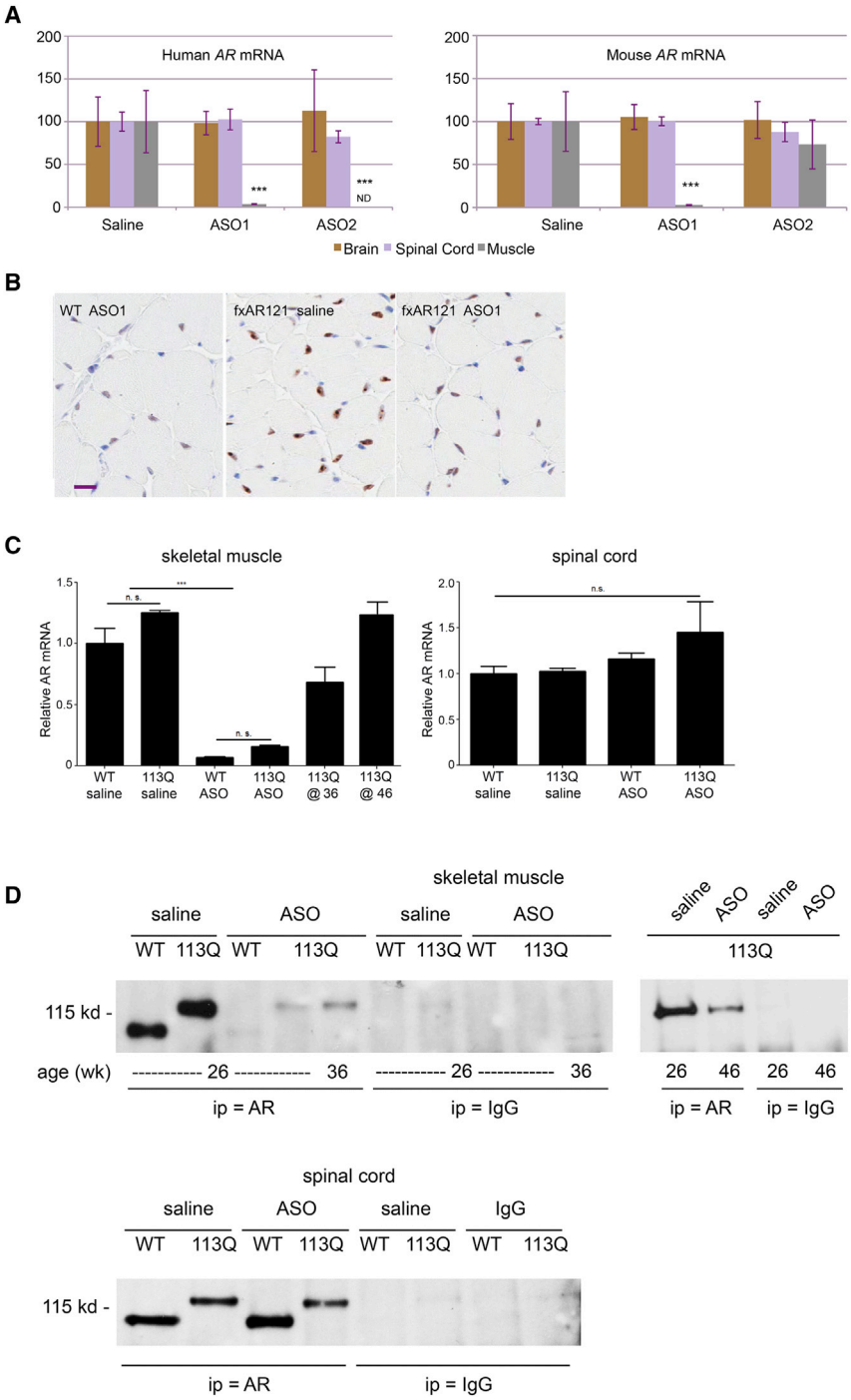

Figure 2. Subcutaneous ASO Administration Suppresses AR Expression in Muscle but Not Spinal Cord

(A) The 11-week-old BAC fxAR121 males (n = 4 per group) received subcutaneous injections of ASOs (50 mg/kg, twice weekly) or saline for 4 weeks. Quadriceps muscle, brain, and spinal cord were harvested 48 hr after the final dose and analyzed for human (left) and mouse (right) AR mRNA levels. Data are mean ± SD. ND, not detected. ***$p < 0.001$ compared to saline treatment.

(B) Wild-type (WT; left) and BAC fxAR121 males (middle and right) received subcutaneous injections of ASO1 (50 mg/kg weekly, starting at 6 weeks) or saline for 4 weeks. The external urethral sphincter muscle was harvested and stained for AR by immunohistochemistry. Scale bar, 15 μm.

(C and D) AR113Q (n = 10 per group) and WT (n = 3 per group) males received subcutaneous injections of ASO1 (50 mg/kg, twice weekly for 4 weeks, and then once weekly) or saline, from 8 until 26 weeks. Quadriceps muscle and spinal cord were harvested at the indicated ages and analyzed for (C) AR mRNA (mean ± SEM) and (D) protein by immunoprecipitation and western blot. ***$p < 0.001$; n.s., not significant.

in mice at 36 weeks of age, 10 weeks after termination of treatment, but was lost at 46 weeks, or 20 weeks off treatment. These findings paralleled changes in polyQ-AR expression (Figures 2C and 2D). ASO1 treatment also diminished the frequency of AR immunoreactive intranuclear inclusions in skeletal muscle nuclei of knockin males (Figure 6C). These inclusions were not detected in quadriceps muscle of treated males at 26 weeks and were present in only occasional nuclei of the levator ani/bulbocavernosus (LA/BC) muscle. Because the LA/BC expresses high levels of AR (Jordan et al., 1997; Monks et al., 2004), intranuclear inclusions were frequent in saline-treated AR113Q males, and their persistence in some nuclei after ASO treatment indicated that a subpopulation was long-lived. Similar findings have been observed following ASO treatment of Huntington disease mice (Kordasiewicz et al., 2012). As with the LA/BC muscle, the external urethral sphincter (EUS) muscle expressed high levels of AR (data not shown) and exhibited more severe and early-onset atrophy than quadriceps muscle (Figure 6D). In BAC fxAR121 males, ASO2 treatment rescued muscle fiber size in both EUS and quadriceps muscles (Figure 6D). In both BAC fxAR121 and AR113Q males, ASO treatment also diminished the levels of acetylcholine receptor-α subunit and myogenin mRNAs, genes that are induced following denervation and are upregulated in SBMA mice (Figures 6E and 6F). In both models, this rescue was partially maintained 6–10 weeks posttreatment.

Finally, to further assess the relative contribution of peripheral polyQ-AR expression to the disease phenotype, we directly compared the efficacy of peripheral versus intraventricular versus combined administration of ASOs in BAC fxAR121 mice. For these experiments, we used a third AR-targeted ASO, ASO3, whose chemistry is well tolerated by mice following

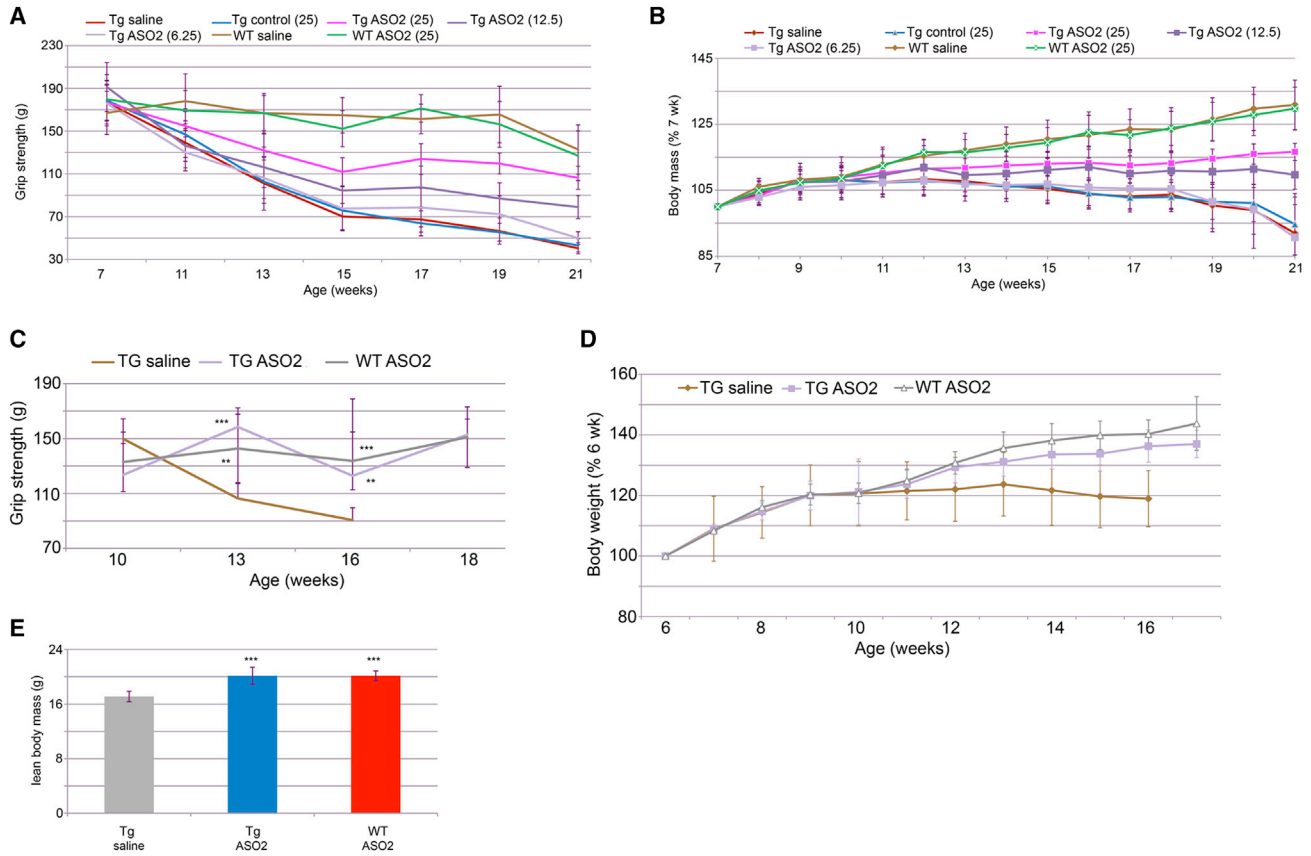

Figure 3. Dose-Dependent Rescue of Grip Strength and Body Mass in BAC fxAR121 Males by ASO2

(A and B) BAC fxAR121 or wild-type (WT) males (n = 10 per group) were treated with increasing doses of ASO2 (6.25–25 mg/kg per week), control ASO, or saline from 7 until 15 weeks. Grip strength (A) and body mass (B) are reported as mean ± SD. Grip strength and body mass of transgenic (Tg) mice treated with ASO2 at 12.5 and 25 mg/kg per week are different from saline treated in weeks 15–21 ($p < 0.05$). Tg mice treated with saline show decreased grip strength compared to WT mice in weeks 11–21 ($p < 0.05$ by ANOVA) and decreased body mass in weeks 12–21 ($p < 0.05$ by ANOVA).

(C and D) BAC fxAR121 or WT males (n = 7–10 per group) received subcutaneous injections of ASO2 (50 mg/kg per week, starting at 6 weeks) or saline for 4 weeks. Age-dependent changes in (C) grip strength and (D) body mass are reported as mean ± SD. In (C), $^{**}p < 0.01$, $^{***}p < 0.001$ compared to saline-treated BAC fxAR121 starting at week 13 by ANOVA. In (D), $p < 0.05$ for ASO2 versus saline-treated Tg mice from weeks 14 to 16 by ANOVA.

(E) BAC fxAR121 or WT males (n = 9–10 per group) received subcutaneous injections of ASO2 (50 mg/kg per week, starting at 6 weeks) or saline for 4 weeks. MRI was performed at 16 weeks and used to determine lean body mass. Data are mean ± SD. $^{***}p < 0.001$ compared to saline-treated BAC fxAR121 by ANOVA.

intraventricular injection (Table S1). We found that a single intraventricular administration of ASO3 (100 μg at 8 weeks) diminished human polyQ-AR mRNA levels in lumbar spinal cord by 60% (Figure 7A). This effect was long-lived and was detected up to 8 weeks after intraventricular administration. Notably, intraventricular delivery did not alter polyQ-AR mRNA levels in quadriceps muscle, which were only diminished in mice receiving subcutaneously delivered ASO2 (Figure 7A). In order to increase the likelihood of detecting an additive benefit from intraventricular administration, we limited the subcutaneous dose to 12.5 mg/kg per week. At this dose, peripheral ASO2 diminished polyQ-AR mRNA expression in muscle by ~60%–70% (Figure 7A) and partially rescued grip strength and survival (Figures 7B and 7C). A single bolus intraventricular administration of ASO3 did not alter grip strength or survival in BAC fxAR121 mice, despite lowering polyQ-AR mRNA expression in lumbar spinal cord (Figures 7B and 7C). Furthermore, combined intraventricular and subcutaneous delivery of ASO was no more effective than subcutaneous delivery alone at rescuing the disease phenotype (Figures 7B and 7C). Altogether, we conclude that peripheral delivery of targeted ASOs suppresses AR expression in skeletal muscle, but not spinal cord, and that this treatment rescues deficits in grip strength, body weight, survival, and skeletal muscle atrophy in two mouse models of SBMA.

DISCUSSION

Our data demonstrate that polyQ-AR suppression outside the CNS is sufficient to ameliorate the disease phenotype in two independent mouse models of SBMA. This strategy is distinct from prior efforts that have focused on targeting polyQ-AR

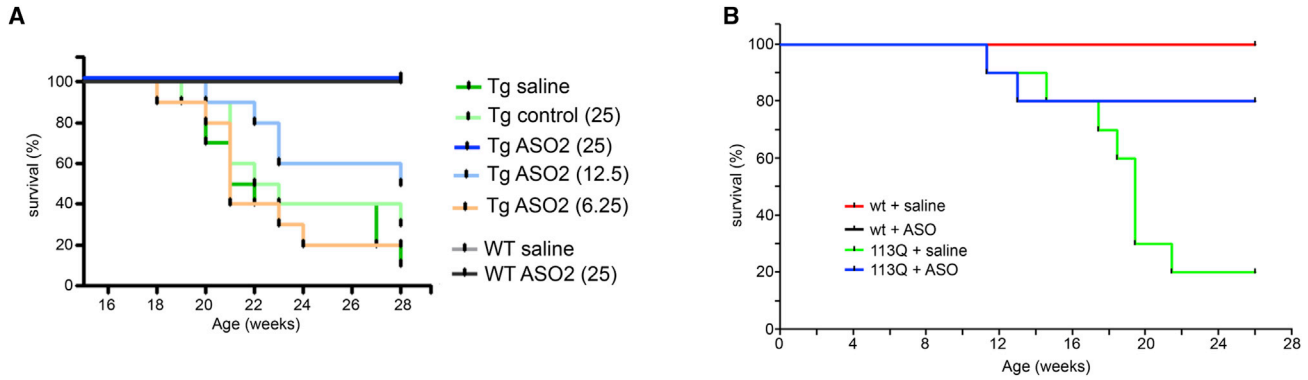

Figure 4. Peripheral PolyQ-AR Suppression Rescues Survival of SBMA Mice

(A) Survival of BAC fxAR121 or wild-type (WT) males (n = 10 per group) treated with increasing doses of ASO2 (6.25–25 mg/kg per week), control ASO, or saline from 7 until 15 weeks. The dark blue/black line depicts overlapping survival curves of WT (saline- and ASO2-treated) and transgenic (Tg) mice treated with ASO2 at 25 mg/kg per week.

(B) Survival of AR113Q (n = 10 per group) and WT (n = 3 per group) males receiving subcutaneous injections of ASO1 or saline from 8 until 26 weeks (as described in Figure 1C). The red line depicts overlapping survival of WT males treated with saline or ASO1. ASO1 treatment significantly extended lifespan of AR113Q males ($p = 0.016$).

toxicity within motor neurons. We show that subcutaneous delivery of ASOs suppresses polyQ-AR expression in skeletal muscle, but not spinal cord, and this rescues deficits in muscle weight, fiber size, and grip strength; reverses changes in muscle gene expression; and extends lifespan of mutant males. Complementary analysis of BAC fxAR121 mice following genetic deletion of the floxed allele specifically in skeletal muscle corroborates our findings (Cortes et al., 2014) and confirms that skeletal muscle is the critical target tissue for this therapeutic intervention.

Our data demonstrate an unexpectedly important contribution of skeletal muscle to the SBMA phenotype. The occurrence of non-cell-autonomous neurotoxicity is an increasingly recognized component of degenerative disorders (Ilieva et al., 2009). For motor neuron diseases, models of familial amyotrophic lateral sclerosis caused by mutant superoxide dismutase 1 have uncovered contributions to pathogenesis from astrocytes, oligodendrocytes, and microglia (Boillée et al., 2006; Di Giorgio et al., 2007; Kang et al., 2013; Lee et al., 2012; Yamanaka et al., 2008). Similarly, models of spinal muscular atrophy have demonstrated important contributions from skeletal muscle (Cifuentes-Diaz et al., 2001; Mutsaers et al., 2011) and have shown efficacy of peripheral gene targeting using ASOs to regulate SMN2 mRNA splicing (Hua et al., 2011). For SBMA, the findings reported here and by Cortes et al. (2014) indicate that peripheral expression of the polyQ-AR in skeletal muscle underlies degenerative changes in the neuromuscular system. This correlates with much higher expression of polyQ-AR protein in skeletal muscle than in spinal cord of SBMA patients (Tanaka et al., 1999). Although the precise mechanism by which skeletal muscle influences disease remains to be defined, impaired trophic support from SBMA muscle may contribute to pathogenesis. Diminished expression of several trophic factors by skeletal muscle in SBMA mouse models has been demonstrated previously, including neurotrophin-4, glial-derived neurotrophic factor, and vascular endothelial growth factor (Sopher et al., 2004; Yu et al., 2006a). Because these and other muscle-derived factors support innervating neurons, their decreased expression could impact the function and viability of lower motor neurons expressing the polyQ-AR as well as their resistance to polyQ toxicity (Jordan and Lieberman, 2008). This model of pathogenesis is consistent with the well-established role of skeletal muscle in maintaining motor neurons (Jessell and Sanes, 2000) and suggests a mechanism whereby the neuromuscular system may be especially vulnerable to toxicity from the polyQ-AR.

The therapeutic benefits documented here following peripheral administration of ASOs provide a compelling rationale for exploring treatments targeted to skeletal muscle in SBMA patients. However, several important questions remain as we work toward translating these findings to patients. The optimal therapeutic dose for alleviating proteotoxicity while maintaining beneficial anabolic effects of AR on skeletal muscle remains to be defined. Figures 1B and 1C show dose-dependent effects on AR mRNA and protein levels over the therapeutic range of ASOs used in these studies, and future work will help optimize this approach to treatment. Importantly, no target-related adverse findings were observed in either WT or SBMA mice following ASO treatment, demonstrating that this treatment approach is feasible, beneficial, and lacking untoward consequences. We recognize that the loss of anabolic effects of AR on skeletal muscle may be more pronounced in SBMA patients than in mice and could necessitate concurrent trophic factor support. Furthermore, we acknowledge that both mouse models exhibit marked skeletal muscle pathology and do not display motor neuron loss, a limitation of the available model systems. Nonetheless, the observations reported here establish a foundation for developing disease-modifying therapies targeted to skeletal muscle and demonstrate the important contribution of peripherally expressed polyQ-AR to SBMA pathogenesis.

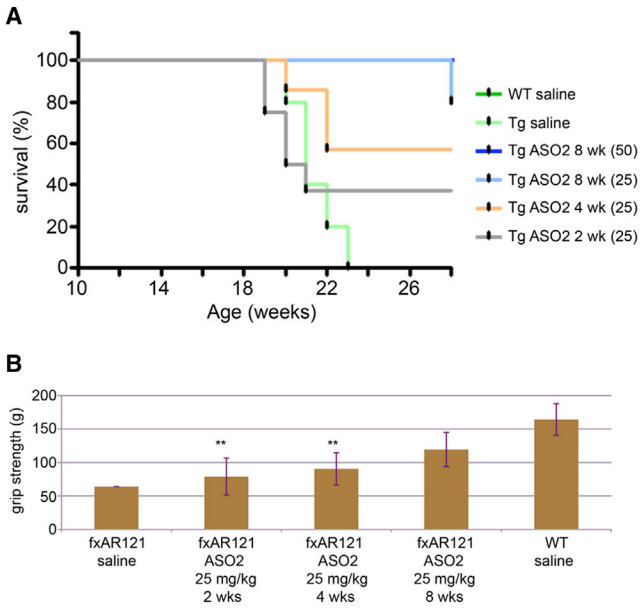

Figure 5. Phenotype Rescue Is Dependent upon Treatment Duration and Is Observed when Treatment Begins at Symptom Onset

BAC fxAR121 or wild-type (WT) males received subcutaneous injections of ASO2 or saline starting at 11 weeks. Mice were treated (n = 6–10 per group) for 8 weeks with 50 mg/kg per week or for 2, 4, or 8 weeks with 25 mg/kg per week.

(A) Survival of BAC fxAR121 (Tg) is significantly extended by ASO treatment ($p < 0.01$). The light-blue line depicts overlapping curves for WT and Tg mice treated with ASO2 at 50 mg/kg per week for 8 weeks and Tg mice treated with ASO2 at 25 mg/kg per week for 8 weeks.

(B) Grip strength at 22 weeks, 4 weeks after final treatment (n = 3–5 per group, except saline-treated BAC fxAR121, where only one mouse survived at this time point).

Data are mean ± SD. **$p < 0.05$ compared to saline-treated WT males.

EXPERIMENTAL PROCEDURES

Mice

Derivation of AR113Q mice with a targeted *Ar* allele containing 113 CAG repeats in exon 1 was described previously (Yu et al., 2006b). Briefly, mice were generated by recombining a portion of human exon 1 (amino acids 31–484) with the mouse *Ar* gene in CJ7 embryonic stem cells. Male chimeras were mated with C57BL/6J females, and females heterozygous for the targeted *Ar* allele were backcrossed to C57BL/6J ten or more generations. BAC fxAR121 mice were derived as described elsewhere (Cortes et al., 2014). Male offspring housed in SPF facilities and maintained on a constant 12 hr light/12 hr dark cycle were used in this study. Subcutaneous administration of ASOs or saline was performed according to the indicated treatment schedules. For intraventricular administration, 8-week-old mice were anaesthetized with 2% isoflurane and held by the head in a stereotaxic instrument. A total of 10 μl of ASO (100 μg) in saline was injected into the right lateral ventricle. The coordinates for injection were 0.3 mm anterior, 1.0 mm lateral, and 3.0 mm ventral from the bregma, as described previously (Sahashi et al., 2013). Body composition was measured by an Echo MRI system (Echo Medical System). Procedures involving mice were approved by the University of Michigan Committee on Use and Care of Animals, in accord with the NIH Guidelines for the Care and Use of Experimental Animals, or by the Isis Pharmaceuticals Institutional Animal Care and Use Committee.

Oligonucleotides

A series of uniform chimeric 16-mer phosphorothioate oligonucleotides containing cEt groups at positions 1–3 and 14–16 targeted to mouse or human *AR* and a control ASO (Table S1) were synthesized and purified on an automated DNA synthesizer using phosphoramidite chemistry, as previously described (Koller et al., 2011). All ASOs were dissolved in PBS and filtered before injections were performed.

RNA Analysis

Total RNA was isolated from tissues of AR113Q knockin males with TRIzol (Invitrogen) according to the manufacturer's instructions. RNA (1 μg) was used to synthesize cDNA with the high-capacity cDNA archive kit (Applied Biosystems). Gene-specific primers (18S rRNA, 4310893E; *Ar*, Mm00442688_m1; *α-acetylcholine receptor*, Mm00431627_m1; *myogenin*, Mm00446194_m1) were purchased from Applied Biosystems, and analyses were performed in duplicate using 10 ng aliquots of cDNA on an ABI 7500 Real Time PCR system. Relative expression levels were calculated by comparison with the expression of 18S rRNA.

BAC fxAR121 tissues were homogenized in a guanidine isothiocyanate solution (Invitrogen) supplemented with 8% 2-mercaptoethanol (Sigma-Aldrich). Total RNA was prepared according to the PureLink Total RNA Purification Kit (Invitrogen). The quantitative RT-PCR analyses were done using a StepOne Real-Time PCR System (Applied Biosystems). The sequences of primers and probe used were as follows: mouse androgen receptor: forward: 5′-CAGCAGAAACGATTGTACCATTG-3′, reverse: 5′- GCTTACGAGCT CCCAGAGTCA-3′, probe: 5′-Fam- AAAATTGCCCATCTTGTCGTCTCCGG-Tamra-3′; human androgen receptor: forward: 5′-GCCCCTGGATGGATAGC TACT-3′, reverse: 5′- CCACAGATCAGGCAGGTCTTC-3′, probe: 5′-Fam-ACTGCCAGGGACCATGTTTTGCCC-Tamra-3′; mouse cholinergic receptor nicotinic, alpha polypeptide1 (Life Technologies) Mm00431627_m1; mouse myogenin (Life Technologies) Mm00446194_m1. PCR results were normalized to total RNA measure by Quant-iT RiboGreen RNA reagent (Molecular Probes).

Immunoprecipitation and Western Blot

Muscle and spinal cord were homogenized in RIPA buffer containing complete protease inhibitor cocktail (Roche) using a motor homogenizer (TH115, OMNI). Lysates were incubated on a rotator at 4°C for 1 hr and then precleared by centrifugation at 13,000 × *g* for 10 min at 4°C. Protein concentration was determined by bicinchoninic acid protein assay (Pierce). Protein lysates (500 μg) were incubated with AR antibody (Millipore, PG-21) or rabbit immunoglobulin G (Santa Cruz Biotechnology) overnight at 4°C and then with protein A beads (Santa Cruz) for 1 hr at 4°C. Beads were washed and the eluate was resolved by 7.5% SDS-PAGE and then transferred to nitrocellulose membranes (Bio-Rad). Blots were probed with AR antibody (Santa Cruz), and proteins were visualized by chemiluminescence (Thermo Scientific).

Muscle Histology and Immunofluorescence Staining

AR113Q skeletal muscle was frozen in isopentane prechilled by liquid nitrogen, sectioned at 5 μm with a cryostat, and stained with hematoxylin and eosin (H&E). For immunofluorescence, frozen sections were stained with an AR antibody (Santa Cruz) and a secondary antibody conjugated to Alexa Fluor 594 (Invitrogen). Confocal images were captured with a Zeiss LSM 510 microscope and a water-immersion lens (×63).

BAC fxAR121 muscle was fixed with 10% neutral buffered formalin, embedded in paraffin, and sectioned at 4 μm. Antigen retrieval was performed by boiling in Thermo citrate buffer (pH 6.0) (Thermo Scientific) for 20 min. Slides were blocked by donkey serum (Jackson ImmunoResearch) for 30 min. The primary antibody (AR: sc-816, Santa Cruz; laminin: ab11575, Abcam) was applied and incubated at room temperature for 1 hr. After three washes in PBS with Tween 20, slides were incubated with donkey anti-rabbit horseradish peroxidase (Jackson ImmunoResearch) at 1:200 for 30 min, then developed with DAB and counterstained with hematoxylin (Surgipath), dehydrated, and mounted.

Muscle Fiber Size Quantification

The cross-sectional diameter of BAC fxAR121 muscle fibers was measured by image analysis after staining with laminin to highlight the muscle membrane. The minimal diameter of each muscle fiber was quantified by the muscle fiber

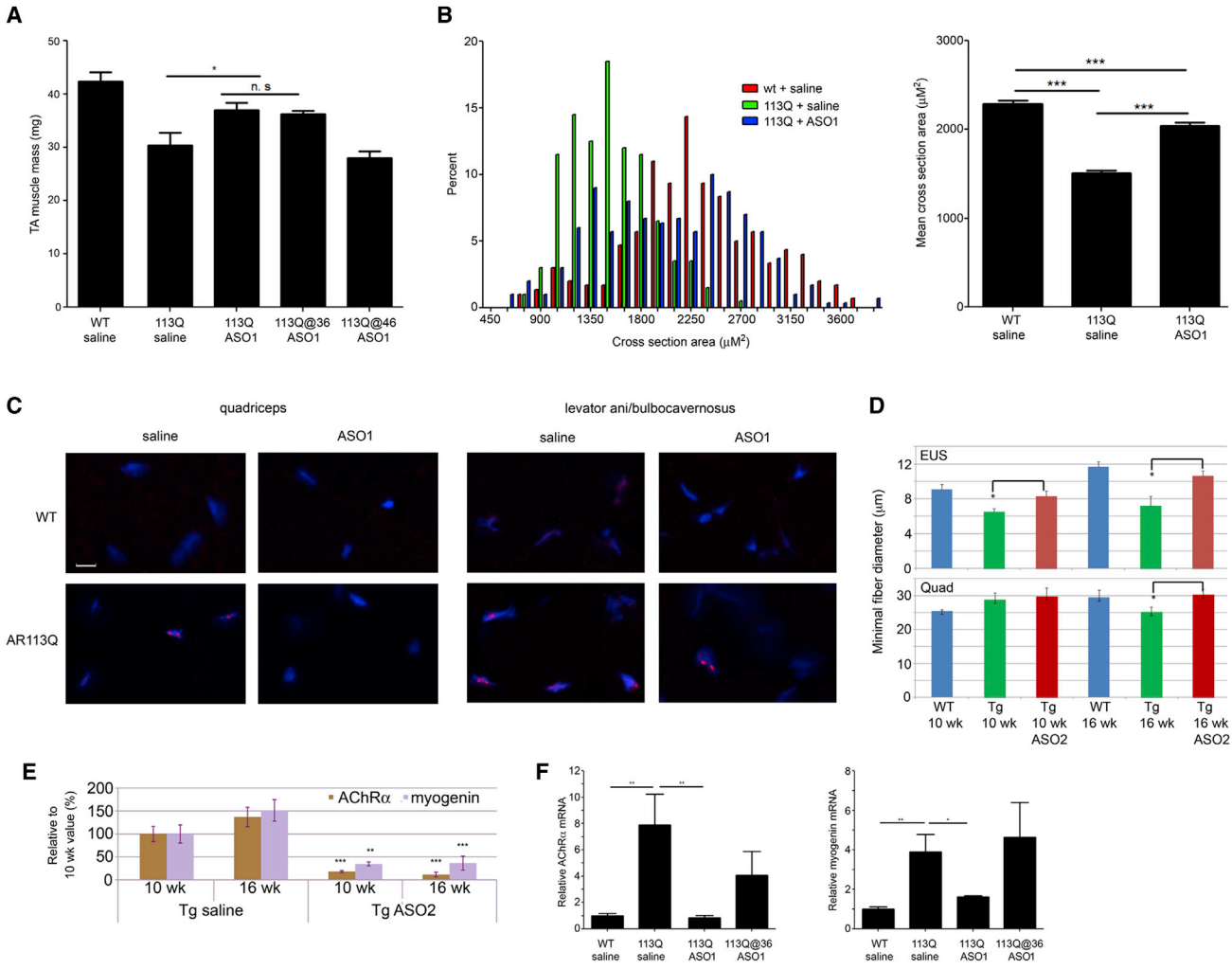

Figure 6. Peripheral ASO Administration Rescues Muscle Atrophy and Gene Expression Changes

(A) Tibialis anterior (TA) muscle mass at 26 weeks from AR113Q or wild-type (WT) males treated with ASO1 or saline (treated as described in Figure 1C) or posttreatment at age 36 or 46 weeks. Data are mean ± SEM. *$p < 0.05$; n.s., not significant.

(B) Quadriceps muscle fiber size distribution (left panel) and mean ± SEM (right panel) from AR113Q or WT males at 26 weeks, treated as described in Figure 1C. ***$p < 0.001$.

(C) AR immunofluorescence (red) of quadriceps and levator ani/bulbocavernosus (LA/BC) muscles of AR113Q and WT males at 26 weeks, treated as described in Figure 1C. DAPI stains nuclei. Scale bar, 10 μm.

(D) External urethral sphincter (upper panel) and quadriceps muscle (lower panel) fiber size were determined from BAC fxAR121 males (n = 4 per group) that received subcutaneous ASO2 (50 mg/kg per week, starting at 6 weeks) for 4 weeks. Muscle was harvested from transgenic (Tg) and WT males at 10 and 16 weeks. Data are mean ± SD. *$p < 0.05$.

(E) BAC fxAR121 males (n = 3–4 per group) received subcutaneous injections of ASO2 (50 mg/kg per week, starting at 6 weeks) or saline for 4 weeks. Quadriceps muscle was harvested at 10 and 16 weeks, and AChR-α and myogenin mRNA expression determined. Data are mean ± SD. **$p < 0.01$, ***$p < 0.001$.

(F) AChR-α and myogenin mRNA expression in quadriceps muscle of AR113Q or WT males at 26 weeks (treated as described in Figure 1C) or following termination of treatment at 36 weeks. Data are mean ± SEM. **$p < 0.01$, *$p < 0.05$.

algorithm (Indica Lab). Frozen sections of AR113Q muscle (5 μm) were stained by H&E, and digital images were captured using a Zeiss Axioplan 2 imaging system. The area of each muscle fiber was defined using Adobe Photoshop CS4, and the pixel number was converted to μm^2 according to scale, as described elsewhere (Yu et al., 2011). A total of 100 adjacent fibers from each section were measured.

Grip Strength

Forelimb strength of BAC fxAR121 mice was measured with a digital grip strength meter that records the maximal strength an animal exerts while trying to resist an opposing pulling force. In brief, each mouse was allowed to grasp the metal rail with its forelimbs and gradually pulled backward in the horizontal plane. The highest reading from five to ten consecutive trials was recorded by a four-channel transducer (TBM4M, World Precision Instruments) using labScribe2 software (Transonic Systems).

Testosterone Levels

Serum was collected by cardiac puncture. Testosterone levels were determined by radioimmunoassay by the Ligand Assay and Analysis Core Facility at the University of Virginia Center for Research in Reproduction.

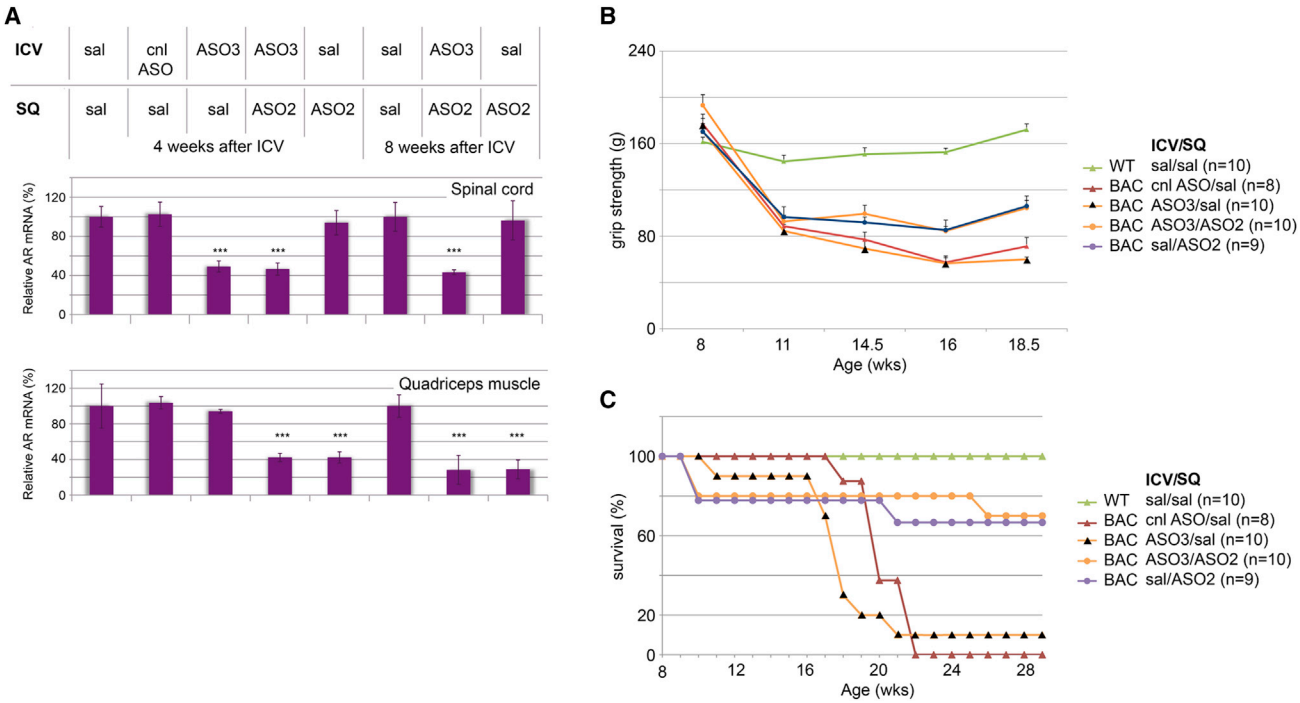

Figure 7. Intraventricular ASO Administration Does Not Provide Added Benefit to BAC fxAR121 Mice Receiving Peripheral ASO

(A) BAC fxAR121 mice were dosed as indicated with saline (sal), intraventricular (ICV) ASO3, or control (cnl) ASO (100 μg at 8 weeks) and subcutaneous (SQ) ASO2 (12.5 mg/kg per week, starting at 8 weeks). Spinal cord and quadriceps muscle were harvested 4 or 8 weeks following ICV administration and analyzed for human AR mRNA levels. Data (mean ± SEM) are reported relative to mice receiving ICV and SQ saline (n = 4 per group). ***$p < 0.001$.

(B and C) Wild-type (WT) or BAC fxAR121 males (n = 8–10 per group) were treated as indicated with saline (sal), intraventricular (ICV) ASO3, or control (cnl) ASO (100 μg at 8 weeks) and subcutaneous (SQ) ASO2 (12.5 mg/kg per week, starting at 8 weeks). Age-dependent changes in grip strength (B) and survival (C) are shown. Data are mean ± SEM.

Statistics

Statistical significance was assessed by an unpaired Student's t test (for pairwise comparisons) or by one-way ANOVA with Newman-Keuls multiple comparison test or Tukey's post hoc test (for multiple comparisons). The distribution of muscle fiber size was analyzed by Mann-Whitney test. Effects on survival were assessed by log-rank analysis. All statistics was performed using Prism 5 or 5.04 (GraphPad Software). p values less than 0.05 were considered significant.

SUPPLEMENTAL INFORMATION

Supplemental Information includes two figures and one table and can be found with this article online at http://dx.doi.org/10.1016/j.celrep.2014.02.008.

ACKNOWLEDGMENTS

This work was supported by the US National Institutes of Health (R01 NS055746 to A.P.L. and R01 NS041648 to A.R.L.) and the Muscular Dystrophy Association (basic research grant to A.R.L. and development award to C.J.C.). S.M., R.P., A.L., S.G., X.X.Y., C.F.B., B.P.M., and G.H. are employees and shareholders of Isis Pharmaceuticals.

Received: August 4, 2013
Revised: January 10, 2014
Accepted: February 5, 2014
Published: April 16, 2014

REFERENCES

Boillée, S., Yamanaka, K., Lobsiger, C.S., Copeland, N.G., Jenkins, N.A., Kassiotis, G., Kollias, G., and Cleveland, D.W. (2006). Onset and progression in inherited ALS determined by motor neurons and microglia. Science *312*, 1389–1392.

Chamberlain, N.L., Driver, E.D., and Miesfeld, R.L. (1994). The length and location of CAG trinucleotide repeats in the androgen receptor N-terminal domain affect transactivation function. Nucleic Acids Res. *22*, 3181–3186.

Cifuentes-Diaz, C., Frugier, T., Tiziano, F.D., Lacène, E., Roblot, N., Joshi, V., Moreau, M.H., and Melki, J. (2001). Deletion of murine SMN exon 7 directed to skeletal muscle leads to severe muscular dystrophy. J. Cell Biol. *152*, 1107–1114.

Cortes, C.J., Ling, S.-C., Ling, G., Hung, G., Tsunemi, T., Ly, L., Tokunaga, S., Lopez, E., Sopher, B.L., Bennet, C.F., et al. (2014). Absence of muscle expression of mutant androgen receptor completely rescues systemic and motor neuron disease phenotypes in a spinal and bulbar muscular atrophy mouse model. Neuron *82*, 295–307.

Di Giorgio, F.P., Carrasco, M.A., Siao, M.C., Maniatis, T., and Eggan, K. (2007). Non-cell autonomous effect of glia on motor neurons in an embryonic stem cell-based ALS model. Nat. Neurosci. *10*, 608–614.

Geary, R.S. (2009). Antisense oligonucleotide pharmacokinetics and metabolism. Expert Opin. Drug Metab. Toxicol. *5*, 381–391.

Hua, Y., Sahashi, K., Rigo, F., Hung, G., Horev, G., Bennett, C.F., and Krainer, A.R. (2011). Peripheral SMN restoration is essential for long-term rescue of a severe spinal muscular atrophy mouse model. Nature *478*, 123–126.

Ilieva, H., Polymenidou, M., and Cleveland, D.W. (2009). Non-cell autonomous toxicity in neurodegenerative disorders: ALS and beyond. J. Cell Biol. *187*, 761–772.

Irvine, R.A., Ma, H., Yu, M.C., Ross, R.K., Stallcup, M.R., and Coetzee, G.A. (2000). Inhibition of p160-mediated coactivation with increasing androgen receptor polyglutamine length. Hum. Mol. Genet. *9*, 267–274.

Jessell, T.M., and Sanes, J.R. (2000). Development. The decade of the developing brain. Curr. Opin. Neurobiol. *10*, 599–611.

Johansen, J.A., Yu, Z., Mo, K., Monks, D.A., Lieberman, A.P., Breedlove, S.M., and Jordan, C.L. (2009). Recovery of function in a myogenic mouse model of spinal bulbar muscular atrophy. Neurobiol. Dis. *34*, 113–120.

Jordan, C.L., and Lieberman, A.P. (2008). Spinal and bulbar muscular atrophy: a motoneuron or muscle disease? Curr. Opin. Pharmacol. *8*, 752–758.

Jordan, C.L., Padgett, B., Hershey, J., Prins, G., and Arnold, A. (1997). Ontogeny of androgen receptor immunoreactivity in lumbar motoneurons and in the sexually dimorphic levator ani muscle of male rats. J. Comp. Neurol. *379*, 88–98.

Kang, S.H., Li, Y., Fukaya, M., Lorenzini, I., Cleveland, D.W., Ostrow, L.W., Rothstein, J.D., and Bergles, D.E. (2013). Degeneration and impaired regeneration of gray matter oligodendrocytes in amyotrophic lateral sclerosis. Nat. Neurosci. *16*, 571–579.

Katsuno, M., Adachi, H., Kume, A., Li, M., Nakagomi, Y., Niwa, H., Sang, C., Kobayashi, Y., Doyu, M., and Sobue, G. (2002). Testosterone reduction prevents phenotypic expression in a transgenic mouse model of spinal and bulbar muscular atrophy. Neuron *35*, 843–854.

Katsuno, M., Adachi, H., Minamiyama, M., Waza, M., Tokui, K., Banno, H., Suzuki, K., Onoda, Y., Tanaka, F., Doyu, M., and Sobue, G. (2006a). Reversible disruption of dynactin 1-mediated retrograde axonal transport in polyglutamine-induced motor neuron degeneration. J. Neurosci. *26*, 12106–12117.

Katsuno, M., Adachi, H., Waza, M., Banno, H., Suzuki, K., Tanaka, F., Doyu, M., and Sobue, G. (2006b). Pathogenesis, animal models and therapeutics in spinal and bulbar muscular atrophy (SBMA). Exp. Neurol. *200*, 8–18.

Kazemi-Esfarjani, P., Trifiro, M.A., and Pinsky, L. (1995). Evidence for a repressive function of the long polyglutamine tract in the human androgen receptor: possible pathogenetic relevance for the (CAG)n-expanded neuronopathies. Hum. Mol. Genet. *4*, 523–527.

Kemp, M.Q., Poort, J.L., Baqri, R.M., Lieberman, A.P., Breedlove, S.M., Miller, K.E., and Jordan, C.L. (2011). Impaired motoneuronal retrograde transport in two models of SBMA implicates two sites of androgen action. Hum. Mol. Genet. *20*, 4475–4490.

Koller, E., Vincent, T.M., Chappell, A., De, S., Manoharan, M., and Bennett, C.F. (2011). Mechanisms of single-stranded phosphorothioate modified antisense oligonucleotide accumulation in hepatocytes. Nucleic Acids Res. *39*, 4795–4807.

Kordasiewicz, H.B., Stanek, L.M., Wancewicz, E.V., Mazur, C., McAlonis, M.M., Pytel, K.A., Artates, J.W., Weiss, A., Cheng, S.H., Shihabuddin, L.S., et al. (2012). Sustained therapeutic reversal of Huntington's disease by transient repression of huntingtin synthesis. Neuron *74*, 1031–1044.

Lee, Y., Morrison, B.M., Li, Y., Lengacher, S., Farah, M.H., Hoffman, P.N., Liu, Y., Tsingalia, A., Jin, L., Zhang, P.W., et al. (2012). Oligodendroglia metabolically support axons and contribute to neurodegeneration. Nature *487*, 443–448.

Lieberman, A.P., and Fischbeck, K.H. (2000). Triplet repeat expansion in neuromuscular disease. Muscle Nerve *23*, 843–850.

Lieberman, A.P., Harmison, G., Strand, A.D., Olson, J.M., and Fischbeck, K.H. (2002). Altered transcriptional regulation in cells expressing the expanded polyglutamine androgen receptor. Hum. Mol. Genet. *11*, 1967–1976.

McCampbell, A., Taylor, J.P., Taye, A.A., Robitschek, J., Li, M., Walcott, J., Merry, D., Chai, Y., Paulson, H., Sobue, G., and Fischbeck, K.H. (2000). CREB-binding protein sequestration by expanded polyglutamine. Hum. Mol. Genet. *9*, 2197–2202.

Mhatre, A.N., Trifiro, M.A., Kaufman, M., Kazemi-Esfarjani, P., Figlewicz, D., Rouleau, G., and Pinsky, L. (1993). Reduced transcriptional regulatory competence of the androgen receptor in X-linked spinal and bulbar muscular atrophy. Nat. Genet. *5*, 184–188.

Monks, D.A., O'Bryant, E.L., and Jordan, C.L. (2004). Androgen receptor immunoreactivity in skeletal muscle: enrichment at the neuromuscular junction. J. Comp. Neurol. *473*, 59–72.

Monks, D.A., Johansen, J.A., Mo, K., Rao, P., Eagleson, B., Yu, Z., Lieberman, A.P., Breedlove, S.M., and Jordan, C.L. (2007). Overexpression of wild-type androgen receptor in muscle recapitulates polyglutamine disease. Proc. Natl. Acad. Sci. USA *104*, 18259–18264.

Morfini, G., Pigino, G., Szebenyi, G., You, Y., Pollema, S., and Brady, S.T. (2006). JNK mediates pathogenic effects of polyglutamine-expanded androgen receptor on fast axonal transport. Nat. Neurosci. *9*, 907–916.

Morishima, Y., Wang, A.M., Yu, Z., Pratt, W.B., Osawa, Y., and Lieberman, A.P. (2008). CHIP deletion reveals functional redundancy of E3 ligases in promoting degradation of both signaling proteins and expanded glutamine proteins. Hum. Mol. Genet. *17*, 3942–3952.

Mutsaers, C.A., Wishart, T.M., Lamont, D.J., Riessland, M., Schreml, J., Comley, L.H., Murray, L.M., Parson, S.H., Lochmüller, H., Wirth, B., et al. (2011). Reversible molecular pathology of skeletal muscle in spinal muscular atrophy. Hum. Mol. Genet. *20*, 4334–4344.

Palazzolo, I., Stack, C., Kong, L., Musaro, A., Adachi, H., Katsuno, M., Sobue, G., Taylor, J.P., Sumner, C.J., Fischbeck, K.H., and Pennuto, M. (2009). Overexpression of IGF-1 in muscle attenuates disease in a mouse model of spinal and bulbar muscular atrophy. Neuron *63*, 316–328.

Ranganathan, S., Harmison, G.G., Meyertholen, K., Pennuto, M., Burnett, B.G., and Fischbeck, K.H. (2009). Mitochondrial abnormalities in spinal and bulbar muscular atrophy. Hum. Mol. Genet. *18*, 27–42.

Rinaldi, C., Bott, L.C., Chen, K.L., Harmison, G.G., Katsuno, M., Sobue, G., Pennuto, M., and Fischbeck, K.H. (2012). Insulinlike growth factor (IGF)-1 administration ameliorates disease manifestations in a mouse model of spinal and bulbar muscular atrophy. Mol. Med. *18*, 1261–1268.

Sahashi, K., Ling, K.K., Hua, Y., Wilkinson, J.E., Nomakuchi, T., Rigo, F., Hung, G., Xu, D., Jiang, Y.P., Lin, R.Z., et al. (2013). Pathological impact of SMN2 mis-splicing in adult SMA mice. EMBO Mol. Med. *5*, 1586–1601.

Seth, P.P., Siwkowski, A., Allerson, C.R., Vasquez, G., Lee, S., Prakash, T.P., Wancewicz, E.V., Witchell, D., and Swayze, E.E. (2009). Short antisense oligonucleotides with novel 2′-4′ conformationaly restricted nucleoside analogues show improved potency without increased toxicity in animals. J. Med. Chem. *52*, 10–13.

Sopher, B.L., Thomas, P.S., Jr., LaFevre-Bernt, M.A., Holm, I.E., Wilke, S.A., Ware, C.B., Jin, L.W., Libby, R.T., Ellerby, L.M., and La Spada, A.R. (2004). Androgen receptor YAC transgenic mice recapitulate SBMA motor neuronopathy and implicate VEGF164 in the motor neuron degeneration. Neuron *41*, 687–699.

Sperfeld, A.D., Karitzky, J., Brummer, D., Schreiber, H., Häussler, J., Ludolph, A.C., and Hanemann, C.O. (2002). X-linked bulbospinal neuronopathy: Kennedy disease. Arch. Neurol. *59*, 1921–1926.

Szebenyi, G., Morfini, G.A., Babcock, A., Gould, M., Selkoe, K., Stenoien, D.L., Young, M., Faber, P.W., MacDonald, M.E., McPhaul, M.J., and Brady, S.T. (2003). Neuropathogenic forms of huntingtin and androgen receptor inhibit fast axonal transport. Neuron *40*, 41–52.

Takeyama, K., Ito, S., Yamamoto, A., Tanimoto, H., Furutani, T., Kanuka, H., Miura, M., Tabata, T., and Kato, S. (2002). Androgen-dependent neurodegeneration by polyglutamine-expanded human androgen receptor in Drosophila. Neuron *35*, 855–864.

Tanaka, F., Reeves, M.F., Ito, Y., Matsumoto, M., Li, M., Miwa, S., Inukai, A., Yamamoto, M., Doyu, M., Yoshida, M., et al. (1999). Tissue-specific somatic mosaicism in spinal and bulbar muscular atrophy is dependent on CAG-repeat length and androgen receptor—gene expression level. Am. J. Hum. Genet. *65*, 966–973.

Thomas, M., Dadgar, N., Aphale, A., Harrell, J.M., Kunkel, R., Pratt, W.B., and Lieberman, A.P. (2004). Androgen receptor acetylation site mutations cause trafficking defects, misfolding, and aggregation similar to expanded glutamine tracts. J. Biol. Chem. *279*, 8389–8395.

Thomas, M., Harrell, J.M., Morishima, Y., Peng, H.M., Pratt, W.B., and Lieberman, A.P. (2006). Pharmacologic and genetic inhibition of hsp90-dependent trafficking reduces aggregation and promotes degradation of the expanded glutamine androgen receptor without stress protein induction. Hum. Mol. Genet. *15*, 1876–1883.

Wang, A.M., Morishima, Y., Clapp, K.M., Peng, H.M., Pratt, W.B., Gestwicki, J.E., Osawa, Y., and Lieberman, A.P. (2010). Inhibition of hsp70 by methylene blue affects signaling protein function and ubiquitination and modulates polyglutamine protein degradation. J. Biol. Chem. *285*, 15714–15723.

Wang, A.M., Miyata, Y., Klinedinst, S., Peng, H.M., Chua, J.P., Komiyama, T., Li, X., Morishima, Y., Merry, D.E., Pratt, W.B., et al. (2013). Activation of Hsp70 reduces neurotoxicity by promoting polyglutamine protein degradation. Nat. Chem. Biol. *9*, 112–118.

Wheeler, T.M., Leger, A.J., Pandey, S.K., MacLeod, A.R., Nakamori, M., Cheng, S.H., Wentworth, B.M., Bennett, C.F., and Thornton, C.A. (2012). Targeting nuclear RNA for in vivo correction of myotonic dystrophy. Nature *488*, 111–115.

Yamanaka, K., Chun, S.J., Boillee, S., Fujimori-Tonou, N., Yamashita, H., Gutmann, D.H., Takahashi, R., Misawa, H., and Cleveland, D.W. (2008). Astrocytes as determinants of disease progression in inherited amyotrophic lateral sclerosis. Nat. Neurosci. *11*, 251–253.

Yu, Z., Dadgar, N., Albertelli, M., Gruis, K., Jordan, C., Robins, D.M., and Lieberman, A.P. (2006a). Androgen-dependent pathology demonstrates myopathic contribution to the Kennedy disease phenotype in a mouse knock-in model. J. Clin. Invest. *116*, 2663–2672.

Yu, Z., Dadgar, N., Albertelli, M., Scheller, A., Albin, R.L., Robins, D.M., and Lieberman, A.P. (2006b). Abnormalities of germ cell maturation and sertoli cell cytoskeleton in androgen receptor 113 CAG knock-in mice reveal toxic effects of the mutant protein. Am. J. Pathol. *168*, 195–204.

Yu, R.Z., Kim, T.W., Hong, A., Watanabe, T.A., Gaus, H.J., and Geary, R.S. (2007). Cross-species pharmacokinetic comparison from mouse to man of a second-generation antisense oligonucleotide, ISIS 301012, targeting human apolipoprotein B-100. Drug Metab. Dispos. *35*, 460–468.

Yu, Z., Wang, A.M., Robins, D.M., and Lieberman, A.P. (2009). Altered RNA splicing contributes to skeletal muscle pathology in Kennedy disease knock-in mice. Dis. Model. Mech. *2*, 500–507.

Yu, Z., Wang, A.M., Adachi, H., Katsuno, M., Sobue, G., Yue, Z., Robins, D.M., and Lieberman, A.P. (2011). Macroautophagy is regulated by the UPR-mediator CHOP and accentuates the phenotype of SBMA mice. PLoS Genet. *7*, e1002321.